

Equatorial upwelling  
Pacific  
Current measurements  
Upwelling équatorial  
Pacifique  
Courantométrie

# Vertical motion in the upper ocean of the equatorial Eastern Pacific

David HALPERN<sup>a\*</sup>, H. Paul FREITAG<sup>b</sup>

<sup>a</sup> School of Oceanography and Department of Atmospheric Sciences, University of Washington, Seattle, WA 98195, USA.

<sup>b</sup> Pacific Marine Environmental Laboratory, National Oceanic and Atmospheric Administration, Seattle, WA 98115, USA.

\* *Present address* : Earth and Space Sciences Division, Jet Propulsion Laboratory, California Institute of Technology, 4800 Oak Grove Drive, Pasadena, CA 91109, USA.

Received 12/3/86, in revised form 19/6/86, accepted 24/6/86.

## ABSTRACT

Using the equation of continuity, computations of the vertical velocity distribution in the upper ocean were made from moored horizontal current measurements recorded for 3 month intervals near 0°, 110°W. A depth-averaged upwelling velocity of  $2.0 \times 10^{-5} \text{ m s}^{-1}$  was characteristic of the Equatorial Undercurrent (EUC). Below the undercurrent, the mean vertical motion was directed downward. In the EUC the nonlinear advection was comparable to the westward force of the prevailing southeasterly winds.

*Oceanol. Acta*, 1987. Proceedings International Symposium on Equatorial Vertical Motion, Paris, 6-10 May 1985, 19-26.

## RÉSUMÉ

Mouvement vertical dans la partie supérieure du Pacifique équatorial Est

L'intensité de la composante verticale de la vitesse du courant dans la partie supérieure de l'océan est calculée à l'aide de l'équation de continuité, à partir des valeurs du courant horizontal enregistrées au point fixe 0°, 110°W pendant des périodes de 3 mois. La valeur moyenne ainsi trouvée pour la composante verticale dans la couche de surface est de  $2,0 \times 10^{-5} \text{ m s}^{-1}$ , intensité caractéristique d'une situation équatoriale en période d'upwelling. En profondeur, au-dessous du sous-courant équatorial (EUC), elle est au contraire dirigée vers le fond. Au sein du sous-courant équatorial, l'intensité de l'advection non linéaire est comparable à celle de la force de frottement exercée en surface par les alizés de Sud-Est.

*Oceanol. Acta*, 1987. Proceedings International Symposium on Equatorial Vertical Motion, Paris, 6-10 May 1985, 19-26.

## INTRODUCTION

Upwelling is a process of vertical motion in the sea whereby subsurface water moves upward toward the surface; downwelling or sinking is the opposite process. Cromwell (1953) suggested that, as a result of Ekman wind-drift theory, easterly (westerly) winds would produce poleward (equatorward) flow near the surface, with upwelling (downwelling) at the equator

resulting from the divergence (convergence). The persistent occurrences of relatively large primary productivity and low sea surface temperature (SST) in a narrow band along the equator are indicators of upward motion.

Measurements of vertical motion are extremely difficult because of the smallness of the speed. In the interior of the oceans' gyres, wind-driven vertical motion beneath the near-surface Ekman layer is

approximately  $10^{-7} - 10^{-6} \text{ m s}^{-1}$  (Stommel, 1964). Near coastal boundaries where upwelling is sometimes a dominant process, vertical velocities as large as  $10^{-4} \text{ m s}^{-1}$  have been estimated (Halpern, 1976). No direct measurements of equatorial vertical motion have yet been made. Upwelling is sometimes inferred from changes in the position of conservative or non-conservative properties such as temperature (e.g., Wyrski, Eldin, 1982). Another technique to determine vertical motion in the upper ocean uses the equation of continuity (e.g., Bubnov, 1987; Hansen, Paul, 1987).

On two occasions, 20 January-24 April 1979 and 9 February-24 June 1981, a triangular array of moored current measurements in the upper ocean near  $0^\circ$ ,  $110^\circ\text{W}$  was used to compute vertical motion from the equation of continuity. Because the design of the 1981 array precluded reliable estimates of vertical motion (to be discussed later), attention will focus upon the 1979 data. Current measurements were made at 6 or 7 depths between 20 and 250 m. The small scale triangular arrays, which had sides of about 100 km, were located about 2 200 km west of the Galapagos Islands and where the ocean depth is 3 700 m.

### OCEANOGRAPHIC CONDITIONS

In the region of our  $0^\circ$ ,  $110^\circ\text{W}$  moorings the SST has: 1) a strong annual cycle, being highest (SST  $\approx 26^\circ\text{C}$ ) in March-April and lowest (SST  $\approx 20-22^\circ\text{C}$ ) in September-October 2) a strong meridional temperature gradient ( $\approx 1^\circ\text{C}/100 \text{ km}$ ) between  $0^\circ$  and  $5^\circ\text{N}$  in September-October but not in March-April; and 3) a strong zonal temperature gradient ( $\approx 1^\circ\text{C}/1 000 \text{ km}$ ) along the equator in September-October but not in March-April (Reynolds, 1982). At  $110^\circ\text{W}$  the mixed layer thickness was  $\approx 20 \text{ m}$ , the thermocline, which is arbitrarily defined as the region between the 15 and  $25^\circ\text{C}$  isotherms where the temperature gradient is about  $0.1^\circ\text{C m}^{-1}$ , occurred between about 25 and 125 m, and from 175 to 300 m there was a thermostad where the gradient was less than  $0.01^\circ\text{C m}^{-1}$ . Thus, our vertical motion estimates were made in a region of large zonal, meridional and vertical temperature gradients which vary throughout the year.

The annual wind stress forcing over the eastern Pacific is neither uniform in space or time (Wyrski, Meyers, 1976). At  $0^\circ$ ,  $110^\circ\text{W}$  the maximum ( $-4.5 \text{ m s}^{-1}$ ) and minimum ( $-2.0 \text{ m s}^{-1}$ ) westward wind speeds occur in September and March, respectively. Meridional and zonal wind components at  $0^\circ$ ,  $110^\circ\text{W}$  are nearly equal, yielding southeast trades.

The annual mean horizontal circulation pattern in the upper ocean at  $0^\circ$ ,  $110^\circ\text{W}$  consists of a thin ( $\approx 20 \text{ m}$ ) westward current near the surface [which is representative of the South Equatorial Current (SEC)], a 175-225 m thick Equatorial Undercurrent (EUC) flowing eastward along the equator in the thermocline, and westward flow below the EUC. Typical annual mean zonal speeds are  $0.05 \text{ m s}^{-1}$  for the surface branch of the SEC,  $1.0 \text{ m s}^{-1}$  for the EUC, and  $< 0.1 \text{ m s}^{-1}$  at 250 m depth (Halpern, 1987 a). The EUC, which is driven by the zonal pressure gradient of sea level produced by the easterly winds, is always present,

except perhaps during El Niño. In contrast to the small annual cycle of the current at the core of the EUC, the zonal flow above 50 m has a very strong annual cycle. At 20 m the monthly averaged flow during March-May is eastward with speeds at  $0.5 \text{ m s}^{-1}$ , while from July to December the current is westward with a speed of about  $0.25 \text{ m s}^{-1}$ . Current oscillations with periods of about 20 days occur along the equator above the thermocline. The amplitude of the meridional current oscillation ( $\approx 0.5 \text{ m s}^{-1}$  at 20 m) was nearly twice as intense as the zonal component. These waves occur seasonally and are more prominent when the surface current is westward.

When the 1979 experiment was made, the large scale oceanographic and meteorological conditions were normal. However, upwelling was at its annual minimum during February, March, and April because easterly winds were at their annual minimum, surface currents flowed eastward, and SST was at its annual maximum.

### MATERIALS AND METHOD

Horizontal current measurements were made with EG & G Sea Link vector-averaging current meters (VACM) suspended beneath tautly moored surface toroidal buoys. Each VACM also recorded temperature. Halpern (1987 b) found virtually identical data recorded by VACM and vector-measuring current meter (VMCM) doublets placed at several depths (as deep as 160 m) on moorings similar to the ones used in 1979. Because the VMCM has smaller potential sources of errors than a VACM (Weller, Davis, 1980), VMCM data are generally considered to be more representative of the true current field; thus, these VACM observations were considered reliable.

Throughout 20 January-2 May 1979 the moored array consisted of four sites located within 100 km of  $0^\circ$ ,  $110^\circ\text{W}$  (Fig. 2 inset). The T1, T2, T3, and T4 moorings each contained VACMs at 20, 50, 100, 150, 200 and 250 m depths. At T1 no data were obtained from the 20 and 250 m current meters because of electronic problems, and the T2 150-m VACM recorded for only 94 days, which defines the length of common record for this analysis. The T3 mooring contained an additional VACM at 75 m which indicated that the core depth of the EUC was approximately 75 m. Because of the inflection point in the zonal current profile at 75 m, the missing T1 20-m data could not be extrapolated from the shear between 50 and 100 m, and the T1 measurements were therefore not used in the computation of the vertical motion.

### IN SITU MEASUREMENTS

Wind measurements were recorded at 3.5 m height at the buoys. The 15-minute east and north wind components were extrapolated to 10-m height assuming a log profile and a von Karman's constant of 0.4. Wind speeds were low, rarely exceeding  $10 \text{ m s}^{-1}$  at 10-m height. The mean ( $\pm$  standard deviation) of the hourly east-west ( $\text{TAU}_x$ ; positive eastward) and north-south ( $\text{TAU}_y$ ; positive northward) components of the wind stress computed from the square law and a drag coefficient of  $1.3 \times 10^{-3}$  were  $-2.0(\pm 1.8) \times$

$\times 10^{-2} \text{ N m}^{-2}$  and  $1.9(\pm 2.1) \times 10^{-2} \text{ N m}^{-2}$ , respectively. The  $314^\circ$  true direction was representative of the southeast trades. The wind stress was not steady, *e.g.*, the mean values and standard deviations were comparable in magnitude. Spectral estimates of the  $\text{TAU}_x$  and  $\text{TAU}_y$  time series with zero mean value and zero least-square linear trend were computed from Cooley-Tukey Fourier transforms using the perfect Daniell window of variable width. On the basis of the spectra, fluctuations at frequencies less than 0.6 cpd were defined as low frequency variations. For each  $\text{TAU}_x$  and  $\text{TAU}_y$  series, the Fourier coefficients were computed, the harmonics with frequencies greater than 0.6 cpd were subtracted, and the residual coefficients retransformed. Time series of the low frequency variations of  $\text{TAU}_x$  and  $\text{TAU}_y$  (Fig. 1) contained fluctuations as large as  $0.1 \text{ N m}^{-2}$ .

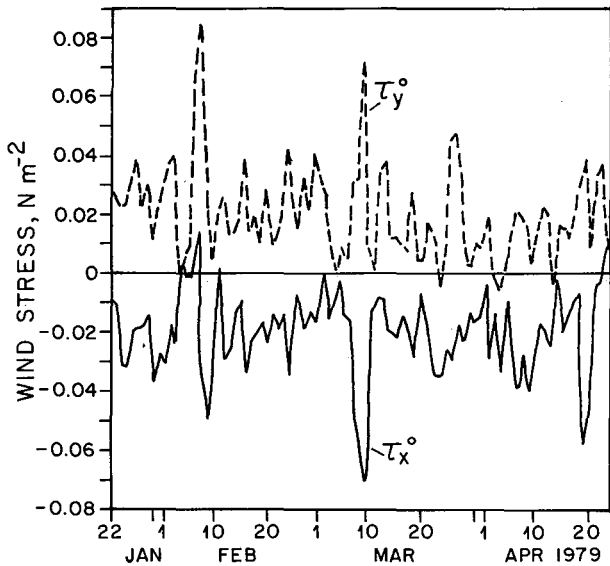


Figure 1  
Low-pass filtered variations of the east-west (solid line) and north-south (dashed line) components of surface wind stress at  $0^\circ, 110^\circ\text{W}$ .

Figure 2 contains the 94-day (20 January-24 April) mean values of the east-west ( $u$ ; positive eastward) and north-south ( $v$ ; positive northward) current components. At the T2, T3, and T4 sites the mean  $u$  component at 20 and 50 m depths were about  $0.18 \text{ m s}^{-1}$  and  $0.87\text{-}0.94 \text{ m s}^{-1}$ , respectively. The maximum mean  $u$  speed ( $1.16 \text{ m s}^{-1}$ ) was measured

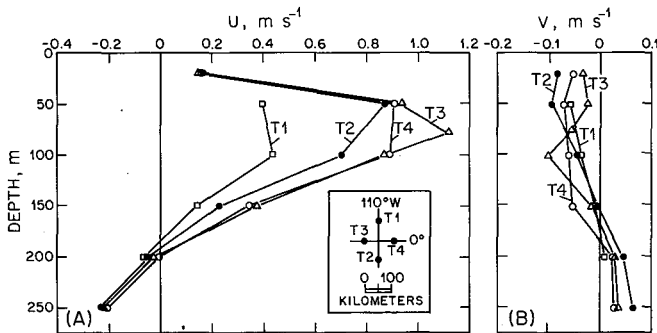


Figure 2  
Vector-mean values of east-west (A) and north-south (B) current components measured from 20 January-24 April 1979 near  $0^\circ, 110^\circ\text{W}$ . Locations of the four surface moorings are shown in the inset diagram in (A).

at 75 m depth, suggesting that depth to be the approximate depth of the core of the EUC. The 94-day mean direction of the  $u$  component changed from eastward to westward between 180 and 200 m. The large difference ( $\approx 0.4 \text{ m s}^{-1}$ ) between the T1 (75 km north of the equator) and T2 (75 km south of the equator) mean  $u$  values at 50 and 100 m indicated that the undercurrent was probably located more often south of the equator. This southward or upwind shift of the EUC is believed to be a nonlinear response of the undercurrent to a southeasterly wind (Cane, 1979), such as observed during this observational period.

The vertical distribution of the mean meridional currents was not consistent with vertical motion resulting from Ekman poleward currents near the surface north and south of the equator and geostrophic equatorward flow into the EUC. It is difficult to measure small mean  $v$  currents in the presence of very strong  $u$  currents and in the presence of large amplitude 20-day meridional current oscillations. At 50 m depth, which was the shallowest level where simultaneous currents were recorded north and south of the equator, the directions of the T1 and T2 mean meridional currents were the same. Also, identical directions of the mean meridional currents at 100 m (and 150 m) at T1 and T2 were not representative of a mean convergent flow pattern beneath the undercurrent core.

The mean  $v$  components were small relative to the  $u$  component (Fig. 2), especially in the region of the EUC. Because  $u$  is large, the errors of the VACM compass and vane direction measurements,  $\pm 6^\circ$  according to manufacturer's specifications, could yield a considerable error in  $v$ . During nearly all of February,  $u > 1.0 \text{ m s}^{-1}$  at 50 and 100 m (Fig. 3).

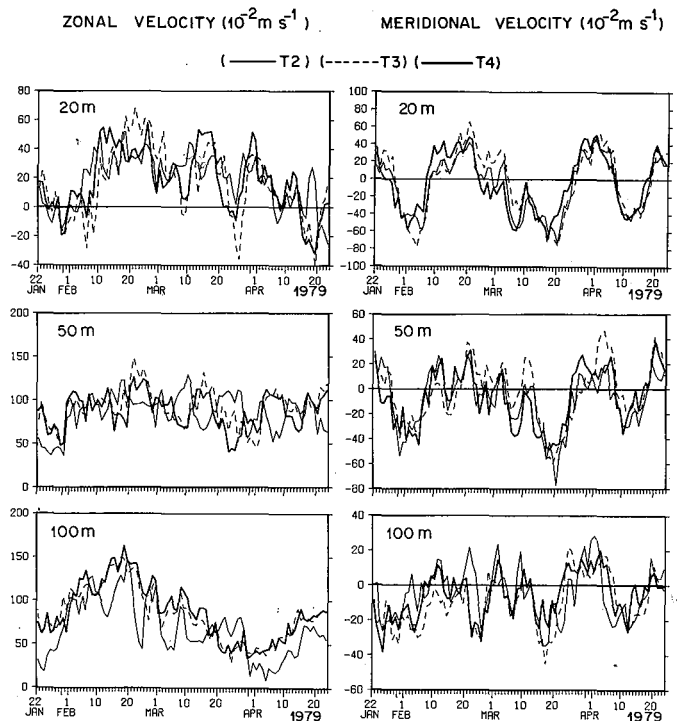


Figure 3  
Low frequency variations of the zonal (positive eastward) and meridional (positive northward) velocity components at 20, 50, and 100 m at T2, T3, and T4 buoy sites.

When  $u = 1.0 \text{ m s}^{-1}$  and  $v = 0.1 \text{ m s}^{-1}$ , then  $s$  (vector-averaged speed) =  $1.01 \text{ m s}^{-1}$  and  $\phi$  (vector-averaged true direction) =  $84^\circ$ . For  $\phi = 84^\circ \pm 6^\circ$ ,  $u$  varies by  $\pm 0.01 \text{ m s}^{-1}$  (or 1%) while the uncertainty of  $v$  is  $\pm 0.11 \text{ m s}^{-1}$  (or 110%).

Spectral estimates of the  $u$  and  $v$  currents contained a statistically significant (at the 95% confidence level) peak only at the semidiurnal tidal frequency. In the computation of the vertical motion from the equation of continuity, the  $u$  and  $v$  time series were low-pass filtered with a cutoff frequency of 0.6 cpd. Inspection of the low-pass filtered time series (Fig. 3) indicated that the low frequency variations of the currents were coherent throughout the array. At frequencies below about 0.1 cpd the currents were coherent at the 95% confidence level.

## VERTICAL MOTION FORMULATION

As a result of Ekman wind-drift, the easterly wind component along the equator would create in the upper layer a northward drift north of the equator and southward drift south of the equator. Upwelling in the upper layer is thus related to the locally wind-forced near-surface divergence, which is partly balanced by a convergence of subsurface geostrophic flow due to the zonal slope of sea level along the equator.

Vertical velocity was computed from the continuity equation:

$$\partial w / \partial z = -(\partial u / \partial x + \partial v / \partial y) \quad (1)$$

where  $x$ ,  $y$  and  $z$  are positive eastward, northward and upwards from the sea surface, and  $w$  (positive upwards) is the vertical velocity. At any two current meter depths the vertical velocities are found by integrating equation (1) along  $z$ . Assuming that the divergence is approximately constant between current meter depths, the vertical velocities at  $z = -h_1$  and  $z = -h_2$ , where  $h_2 > h_1$ , are given by

$$\begin{aligned} w(z = -h_1) - w(z = -h_2) &= \\ &= - \int_{-h_2}^{-h_1} (\partial u / \partial x + \partial v / \partial y) dz \quad (2) \end{aligned}$$

The vertical velocity at the surface is assumed to be zero [i.e.,  $w(z = 0) = 0$ ]. This assumption is reasonable because the vertical motion computed from sea level measurements is much less than the vertical velocity expected to be found in the upper ocean. During January-April 1979, daily sea level at Santa Cruz Island ( $0^\circ 27' \text{S}$ ,  $90^\circ 17' \text{W}$ ) in the Galapagos Archipelago was steady to within  $\pm 2.5 \text{ cm}$  (Wyrski, pers. comm.), and the computed maximum vertical velocity of the sea surface for time scales greater than 2-3 days was about  $1 \times 10^{-7} \text{ m s}^{-1}$ , which is about 1% of the vertical motion in the equatorial upper ocean. Therefore, at 20 m depth the vertical velocity is

$$w(z = -20 \text{ m}) = \int_{-20 \text{ m}}^0 (\partial u / \partial x + \partial v / \partial y) dz \quad (3)$$

Because the mean shear between 20 and 50 m was nearly the same at T2, T3, and T4 (Fig. 2), the surface

currents were extrapolated from the 20 m currents and the 20-50 m shear. At 50 m the integration constant is equal to  $w$  ( $z = -20 \text{ m}$ ); at 100 m,  $w$  ( $z = -50 \text{ m}$ ) is used; and so on. With this procedure the vertical velocity at each current meter level was computed.

Between two current meter levels, the  $x$ -term of the horizontal divergence of the vertically integrated transport was equal to

$$\partial \left( \int u dz \right) / \partial x = \left[ \left( \int u dz \right)_{T4} - \left( \int u dz \right)_{T3} \right] / 112 \text{ km} \quad (4)$$

where  $(\int u dz)_{T4}$  was the zonal transport per unit meridional width at T4, and so forth. The  $\int u dz$  between 50 and 100 m was computed at T3 using the 75-m measurements. At T4 where there were no 75-m observations, a 75-m  $u$  time series at T4 was created from the T3 shear between 50 and 75 m. The  $y$ -term of the divergence was equal to

$$\partial \left( \int v dz \right) / \partial y = \left[ \left( \int v dz \right)_{T4/T3} - \left( \int v dz \right)_{T2} \right] / 73 \text{ km} \quad (5)$$

where

$$\left( \int v dz \right)_{T4/T3} = \left[ \left( \int v dz \right)_{T4} + \left( \int v dz \right)_{T3} \right] / 2 \quad (6)$$

The principal error in calculating vertical velocities arises from errors in measuring the horizontal velocities. If  $w_{\text{ERR}}$  is the uncertainty in the vertical velocity due to measurement error,  $e$ , of the horizontal velocity vector,  $v$ , then equation (1) can be written as

$$\partial (w + w_{\text{ERR}}) / \partial z = (1/A) \oint (v + e) \cdot n dS \quad (7)$$

where  $A$  is the area enclosed by the buoy array and  $n$  is the outward unit normal vector of the line element  $dS$ . Therefore,

$$\partial w_{\text{ERR}} / \partial z = (1/A) \oint e \cdot n dS = eC/A \quad (8)$$

where  $C$  is the perimeter of the triangular buoy array. For a layer of thickness  $H$ , the vertical velocity error is  $eCH/A$ . The accuracy of our upper ocean current measurements is probably  $0.01 \text{ m s}^{-1}$  (Halpern, 1987 b). With  $e = 0.01 \text{ m s}^{-1}$ ,  $A = 4.0 \times 10^9 \text{ m}^2$ ,  $H = 20 \text{ m}$ , and  $C = 2.9 \times 10^5 \text{ m}$ , then  $w_{\text{ERR}} = 1.5 \times 10^{-5} \text{ m s}^{-1}$ ; for  $H = 50 \text{ m}$ ,  $w_{\text{ERR}} = 3.5 \times 10^{-5} \text{ m s}^{-1}$ . As will be shown, these uncertainty values are approximately the same magnitude as the vertical motions computed from the observations.

## RESULTS

The distribution of the mean values of  $w$  is shown in Figure 4. While the uncertainty caused by the accuracy

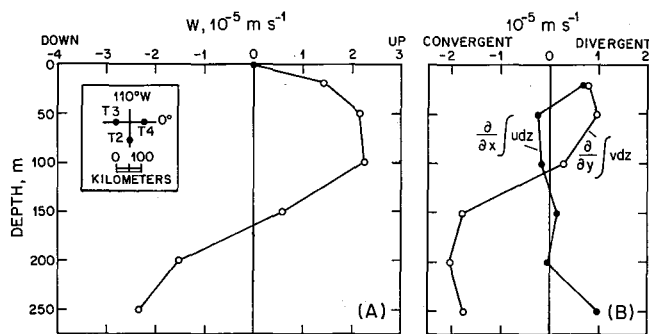


Figure 4

A) Mean vertical velocity profile computed from the continuity equation using moored current measurements. B) Vertical distributions of the  $x$ - and  $y$ -terms of the continuity equation.

of the instrumentation is as large as the computed vertical velocity, the results, several of which are consistent with previous notions, are instructive for planning experiments to estimate vertical motion near within the equator.

Maximum upwelling of  $2.2 \times 10^{-5} \text{ m s}^{-1}$  occurred at 50 and 100 m, *i.e.*, 25 m above and below the EUC core speed, the transition from upwelling to sinking motions was at 175 m, and the average upwelling speed between 20 and 150 m was  $1.8 \times 10^{-5} \text{ m s}^{-1}$ . At 200 and 250 m the mean vertical motion was directed downward. This local distribution of  $w$  was remarkably similar to Bryden and Brady's (1985) estimate computed from a diagnostic model for the  $5^{\circ}\text{N}$ - $5^{\circ}\text{S}$ ,  $150^{\circ}\text{W}$ - $110^{\circ}\text{W}$  region. Our vertical velocity distribution also resembled the one computed by Bubnov (1987), who applied the continuity equation to moored current measurements made along  $163^{\circ}\text{W}$  and  $167^{\circ}\text{W}$  from  $1^{\circ}30'\text{N}$  and  $1^{\circ}30'\text{S}$  during a 28-day period in February-March 1980. It was satisfying that the bottom depth of the upwelling zone was about the same that Fine *et al.* (1983) found from tritium data.

If the  $2.0 \times 10^{-5} \text{ m s}^{-1}$  vertically-averaged upwelling velocity computed at  $110^{\circ}\text{W}$  was continuous along the equator from  $180^{\circ}$  to  $90^{\circ}\text{W}$  and throughout the  $2^{\circ}$  latitudinal width of the undercurrent, then the amount of water upwelled from the thermocline would be  $40 \times 10^6 \text{ m}^3 \text{ s}^{-1}$  (*i.e.*, 40 Sverdrups). Our estimate is an approximate one because it neglects the westward increase of the easterly wind stress and assumes constant upwelling throughout the latitudinal extent of the undercurrent instead of decreasing north and south of the undercurrent core. This value is 20% less than Wyrski's (1981) estimate of upwelling determined from heat, mass, and salt budgets between  $5^{\circ}\text{N}$  and  $5^{\circ}\text{S}$  and from  $90^{\circ}\text{W}$  to the dateline. When the amount of upwelling is computed over the  $80^{\circ}\text{W}$  to  $130^{\circ}\text{W}$  region, our estimate is 25% less than Hansen and Paul's (1987) result determined from the horizontal divergence of drifting buoys. During 8 March to 2 June 1980 when simultaneous current measurements were made at  $152^{\circ}\text{W}$  and  $110^{\circ}\text{W}$  (Knox, Halpern, 1982), the mean transport of the EUC decreased by 7 Sverdrups from  $152^{\circ}\text{W}$  to  $110^{\circ}\text{W}$ . It is tempting to speculate that the loss of undercurrent water was caused primarily by upwelling.

Circulation models of wind-driven Ekman divergence at the equator indicate that at near-equatorial sites the near-surface meridional flow is directed poleward and

below the undercurrent core the flow is equatorward. At 20 m depth the  $x$ - and  $y$ -terms of the divergent motion were equal (Fig. 4). Below the depth of maximum undercurrent flow, the meridional term of the mean divergence was dominant, *i.e.*,  $|\partial v/\partial y| > |\partial u/\partial x|$ , and furthermore was negative, indicating convergent flow. Federov's (1975) model of equatorial upwelling postulates that the level of maximum equatorward flow and maximum eastward current coincide and that the upward motion is a maximum at the depth where  $u = 0$  (*i.e.*, at the bottom of the EUC) and where  $v = 0$ . In contrast to this model's results, the observations indicated that below the surface  $w$  and  $v$  were both zero at the same depth, and  $w$  was maximum where  $u$  was also maximum.

The EUC flows down an eastward pressure gradient established by water piled up on the western side of the ocean by easterly winds. Halpern (1980) reported that in the central Pacific the zonal pressure gradient force ( $-4.5 \times 10^{-7} \text{ m s}^{-2}$ ) was more than twice as large as the force of the prevailing westward winds ( $-2.2 \times 10^{-7} \text{ m s}^{-2}$ ), indicating that the magnitude of other terms in the momentum equation may be significant. Above and below the undercurrent core depth (*i.e.*, at 50 and 100 m) the nonlinear advective terms were:  $u(\partial u/\partial x) = -0.5 \times 10^{-7} \text{ m s}^{-2}$ ,  $v(\partial v/\partial y) = -0.3 \times 10^{-7} \text{ m s}^{-2}$ ,  $w(\partial w/\partial z) = -3.0 \times 10^{-7} \text{ m s}^{-2}$ . The vertical momentum advection term was comparable to the wind stress, indicating the importance of including nonlinear dynamics in studies of the undercurrent. At the bottom of the EUC near 200 m depth the dynamics of the flow were essentially linear.

At each level the low frequency variations of the vertical motions were large compared to the mean value. The temporal variability, as measured by the standard deviations, increased with depth. The standard deviations of the vertical velocities at 20, 100 and 250 m were  $4 \times 10^{-5}$ ,  $14 \times 10^{-5}$  and  $18 \times 10^{-5} \text{ m s}^{-1}$ , respectively. On numerous occasions the low-pass filtered values of  $w$  at 20 and 50 m exceeded single estimates made in the Pacific at  $\approx 30$  m depth by Federov (1975) and others; other instantaneous estimates must be considered as random samples from a highly variable field and their representativeness of average conditions is questioned.

Wind measurements recorded at 3.5 m height at the buoy sites were used to examine the relationship between variations of the near-surface meridional current and zonal wind stress. No significant (at the 95% confidence level) coherence was found between hourly values of  $\text{TAU}_x$  at T4 and the 20-m  $v$  current at the T2 site south of the equator. Nor was statistically significant coherence found between  $\text{TAU}_x$  and  $w$  at 20 m.

## DISCUSSION

### Temperature Variations

The persistent occurrences of relatively large primary productivity and low SST in a narrow band along the equator in the central and eastern Pacific are thought to be related to the upwelling of cold, nutrient-rich

waters from the thermocline. However, at 20 m depth no apparent relationship was found between temperature observations and computed vertical motion (Fig. 5). The observed temperature rise during the 94-day period was coincident with mean upward motion, indicating that the role of local wind-forced upwelling in changing near-surface temperature was not the dominant process. Furthermore, no statistically significant (at the 95% confidence level) coherence was found between the 20-m temperature measurements and the computed vertical motion at 20 m. For wind fluctuations with time scales less than about 5 days, the divergence of the wind-driven motion in the surface layer excites short Kelvin waves (Philander, Pacanowski, 1981 *a*), which, combined with diurnal-period mixing events in the uppermost 50-75 m (Gregg *et al.*, 1985; Moum, Caldwell, 1985), destroys the local coherence, increasing the difficulty of establishing statistically significant correlations between vertical motion and temperature changes with relatively short time series.

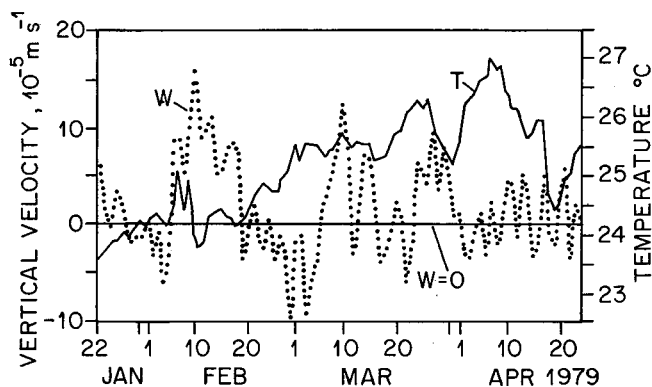


Figure 5

Low-pass filtered time variations of the T4 and T2 averaged 20 m temperature and 20 m vertical velocity.

Upwelling and downwelling events, defined as 5-7 day bursts of vertical motion when  $|w| > 10 \times 10^{-5} \text{ m s}^{-1}$  (or  $\approx 9 \text{ m per day}$ ), may be associated with discernible temperature changes. Wyrtki and Eldin (1982) reported upwelling events with speeds of at least 3 m/day from analyses of temperature data. Figure 5 shows the occurrence of three upwelling events (10 February, 10 and 25 March) and one downwelling event on 27 February. The 10 February event was associated with a burst of westward wind stress (Fig. 1). While a drop in temperature was associated with two of the upwelling events, the 10 March event, which was associated with a strong burst of westward winds (Fig. 1), did not seem to perturb the temperature (Fig. 5). The 5 April temperature maximum and the 20 February to 5 March temperature rise corresponded to reduced upward motion. A comparison of the variations of wind stress, 20-m temperature, and 20-m vertical motion does not lead to definitive relationships between these parameters.

During the 94 day observational interval the temperature at 20 m increased by about 3°C and the local time rate of temperature change,  $\partial T/\partial t$ , was  $3.5 \times 10^{-7} \text{ }^\circ\text{C s}^{-1}$ . With mean values of  $w$  and  $\partial T/\partial z$  of  $1.5 \times 10^{-5} \text{ m s}^{-1}$  and  $5 \times 10^{-2} \text{ }^\circ\text{C m}^{-1}$ , the

mean vertical advection of temperature,  $w(\partial T/\partial z)$ , was  $7.5 \times 10^{-7} \text{ }^\circ\text{C s}^{-1}$ , about two times the time rate of temperature change. That  $\partial T/\partial t$  and  $w(\partial T/\partial z)$  were both positive is the mathematical representation that the near-surface temperature increase was not caused by upward movement of the thermocline. Moored temperature and current measurements made at  $0^\circ, 110^\circ\text{W}$  since 1980 indicated clearly that the 3°C warming observed near the surface from February to May was one portion of the annual cycle and was typically associated with a change in the zonal current component from  $-0.25 \text{ m s}^{-1}$  to  $0.5 \text{ m s}^{-1}$  (Halpern, 1987 *a*). The February to May warming is likely due to zonal advection of heat from the west and to reductions of latent heat flux and upwelling arising from the weaker easterly winds during these months compared to the remainder of the year. Our observational period was not optimal *vis-à-vis* estimation of upwelling: September-October, when zonal winds are strongest and SST is lowest, would have been a more appropriate time.

Reynolds' (1982) maps of SST reveal that the axis of cold water in the eastern Pacific does not occur along the equator. In the region  $120^\circ\text{W}$  to  $90^\circ\text{W}$  the coldest water is usually found 2-3° south of the equator. Although it is uncertain whether maximum upwelling velocities at the equator because of Ekman divergence or over the axis of the EUC, which at  $110^\circ\text{W}$  is shifted slightly south of the equator, it is reasonable to assume that neither process would yield significant upwelling motion as far south as 2-3°S. Philander and Pacanowski's (1981 *b*) suggest that the meridional wind component is mainly responsible for the cold water observed a few degrees south of the equator.

### The 1981 Experiment

Another occasion to compute vertical velocities at  $0^\circ, 110^\circ\text{W}$  using the equation of continuity occurred during 9 February to 24 June 1981. The primary difference between the shape of the 1981 triangular array (Fig. 6 inset), which consisted of moorings 75 km north (T14) and south (T16) of the equator and a mooring on the equator (T15), and the 1979 array was the symmetry about the equator in 1981. The mean zonal and meridional currents in 1981 (Fig. 6) were very similar to the 1979 observations, including identical meridional directions at each level north and south of the equator, an undercurrent depth at 75 m, a maximum undercurrent speed of about  $1.18 \text{ m s}^{-1}$ , and a southward shift from the equator of the mean position of the undercurrent. However, the mean vertical velocities in 1981 increased monotonically with depth (Fig. 6), in contrast to our previous result. This situation was puzzling. That the mean vertical velocities computed from the 1979 T1, T2 and T4 array, which was also symmetrical about the equator (see Fig. 2 inset), also increased monotonically with depth below 50 m, where  $w$  was defined to be zero, suggested that the position of the triangular array relative to the equator affected the estimation of  $w$ . Because of the large meridional gradient of the zonal

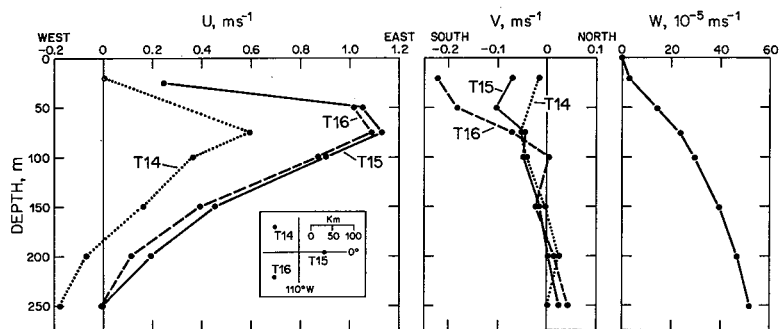


Figure 6

Vector-mean values of east-west, north-south, and vertical components of velocity at  $0^\circ$ ,  $110^\circ\text{W}$  during 9 February to 24 June 1981. Locations of moorings shown in inset.

current in the EUC, the  $\partial u/\partial x$ -term is overestimated when only one element of the triangular buoy array is on the equator. Thus, the 1981 array at  $110^\circ\text{W}$  was poorly designed to estimate equatorial vertical motion in the upper ocean. This situation was confirmed by Knox (pers. comm.) who computed a vertical velocity profile similar to the one shown in Figure 6 using data from a  $0^\circ$ ,  $152^\circ\text{W}$  triangular array similar to the 1981 experiment.

## CONCLUSIONS

- 1) The 94-day averaged upwelling velocity at  $0^\circ$ ,  $110^\circ\text{W}$  computed from a triangular array of horizontal current measurements was equivalent to within 50 % of other estimates determined by different techniques and/or types of data, indicating the establishment of a climatological-mean value of equatorial upwelling of  $1 - 3 \times 10^{-5} \text{ m s}^{-1}$ .
- 2) Large time variations of the computed vertical motion indicated that single estimates might not be representative of the mean condition.
- 3) Relationships between fluctuations of temperature and vertical velocity at 20 m and surface wind stress for time scales less than about 5 days were not very strong, though some agreement existed at longer time scales.
- 4) Care must be exercised in the design of a moored array to estimate vertical motion from the continuity

equation. Estimates of  $\intudz$  at the equator should be avoided using data recorded north and south of the equator because of the strong north-south gradients of  $u$ .

5) For reasons stated in the Introduction, the optimum time to estimate equatorial upwelling at  $110^\circ\text{W}$  is during July to November when the surface current and wind are directed westward with maximum speeds and SST is minimum. Because the horizontal and vertical currents of the upper ocean along the equator respond to all characteristics of the local and far-field surface wind field (Philander, Pacanowski, 1981 a), the January-April 1979 observations and subsequent computation of vertical motion are probably not representative of the annual cycle.

## Acknowledgements

We thank Mark Cane, Robert Knox, George Philander, and Ed Sarachik for comments on an early version of the manuscript. These measurements were obtained as a result of the diligence and hard work of many people, especially Douglas Fenton and Andrew Shepherd. Support by NOAA (EPOCS Grant No. 8C692002) and by NSF (Grant No. OCE-8521510) is gratefully acknowledged. Contribution No. 1690 of the School of Oceanography, University of Washington, and Contribution No. 559 of the NOAA/ERL Pacific Marine Environment Laboratory.

## REFERENCES

- Bryden H. L., Brady E. C., 1985. Diagnostic model of the three-dimensional circulation in the upper equatorial Pacific Ocean, *J. Phys. Oceanogr.*, **15**, 1255-1273.
- Bubnov V. A., 1987. Vertical motions in the central equatorial Pacific, *Oceanol. Acta, Proc. Inter. Symp. on equatorial vertical motion*, this vol., 15-17.
- Cane M. A., 1979. The response of an equatorial ocean to simple wind stress patterns: II. Numerical results, *J. Mar. Res.*, **37**, 253-299.
- Cromwell T., 1953. Circulation in a meridional plane in the central equatorial Pacific, *J. Mar. Res.*, **12**, 196-213.
- Federov K. N., 1975. Estimation of vertical velocity in equatorial upwelling, *Trudy, Institute of Oceanology ANSSR*, **102**, 41-46.
- Fine R. A., Peterson, W. H., Rooth C. G. H., Ostlund H. G., 1983. Cross equatorial tracer transport in the upper waters of the Pacific Ocean, *J. Geophys. Res.*, **88**, 763-769.
- Gregg M. C., Peters H., Wesson J. C., Oakey N. S., Shay T. J., 1985. Intensive measurements of turbulence and shear in the equatorial undercurrent, *Nature*, **318**, 140-144.
- Halpern D., 1976. Structure of a coastal upwelling event observed off Oregon during July 1973, *Deep-Sea Res.*, **23**, 495-508.
- Halpern D., 1980. A Pacific equatorial temperature section from  $172^\circ\text{E}$  to  $110^\circ\text{W}$  during winter and spring 1979, *Deep-Sea Res.*, **27**, 931-940.
- Halpern D., 1987 a. Observations of annual and El Niño thermal and flow variations at  $0^\circ$ ,  $110^\circ\text{W}$  and  $0^\circ$ ,  $95^\circ\text{W}$  during 1980-1985, *J. Geophys. Res.*, **92**, 8197-8212.
- Halpern D., 1987 b. Comparison of upper ocean VACM and VMCM observations in the equatorial Pacific, *J. Ocean. Atmos. Technol.*, **4**, 84-93.
- Hansen D. V., Paul C. A., 1987. Vertical motion in the Eastern

equatorial Pacific inferred from drifting buoys, *Oceanol. Acta, Proc. Inter. Symp. on equatorial vertical motion*, this vol., 27-32.

**Knox R. A., Halpern D.**, 1982. Long range Kelvin wave propagation of transport variations in Pacific Ocean equatorial currents, *J. Mar. Res.*, Suppl., **40**, 329-339.

**Moum J. N., Caldwell D. R.**, 1985. Local influences on shear-flow turbulence in the equatorial ocean, *Science*, **230**, 315-316.

**Philander S. G. H., Pacanowski R. C.**, 1981 a. Response of equatorial oceans to periodic forcing, *J. Geophys. Res.*, **86**, 1903-1916.

**Philander S. G. H., Pacanowski R. C.**, 1981 b. The oceanic response to cross-equatorial winds (with application to coastal upwelling in low latitudes), *Tellus*, **33**, 201-210.

**Reynolds R. W.**, 1982. A monthly averaged climatology of sea

surface temperature. NOAA Technical Report NWS 31, National Meteorological Center, Silver Spring, Maryland, 35 pp.

**Stommel H.**, 1964. Summary charts of the mean dynamic topography and current field at the surface of the ocean, and related functions of the mean wind-stress, in: *Studies on Oceanography*, University of Washington Press, Seattle, 53-58.

**Weller R. A., Davis R. E.**, 1980. A vector-measuring current meter, *Deep-Sea Res.*, **27**, 565-582.

**Wyrtki K.**, 1981. An estimate of equatorial upwelling in the Pacific, *J. Phys. Oceanogr.*, **11**, 1205-1214.

**Wyrtki K., Eldin G.**, 1982. Equatorial upwelling events in the central Pacific, *J. Phys. Oceanogr.*, **12**, 984-988.

**Wyrtki K., Meyers G.**, 1976. The trade wind field over the Pacific Ocean, *J. Appl. Meteorol.*, **15**, 698-704.